Advance Researches in Civil Engineering
ISSN: 2645-7229, Vol.4, No.2, pages: 24-43

Research on the Adhesion and Self-healing Properties of Bio-asphalt Based on Molecular Simulation

Yuan Fu [1], Meng Wu [2], Tianqing Hei [2], Zezhen Dong [2], Jianying Hu [2], Weiguang Zhang [2*]

[1] Highway Administration of Shanxi Province, 030006, Taiyuan, China

[2] School of Transportation, Southeast University, 211189, Nanjing, China

(wgzhang@seu.edu.cn)

(Date of received: 01/03/2022, Date of accepted: 30/05/2022)

ABSTRACT

At present, the extraction of new bio-asphalt materials from renewable energy sources has become the focus of research in the field of pavement engineering. Bio-asphalt has the characteristics of wide source, low cost, green, pollution-free and is also renewable. With the expansion of the application range of bio-asphalt, its adhesion to aggregates and the healing properties after damage have received extensive attention. In this paper, the bio-asphalt-aggregate adhesion and healing behaviors were evaluated and compared using molecular dynamics approaches. Firstly, the molecular models of vegetable oil bio-asphalt and waste edible oil were established, and the two bio-asphalt molecular models were verified according to the physical quantities such as density, viscosity, cohesive energy density (CED), glass transition temperature and solubility parameter. Then, the bio-asphalt-aggregates interlayer model was established, and the adhesion energy and the energy ratio (ER) value under water conditions were calculated and analyzed using energy theory. A bio-asphalt self-healing model was established, and concentration distribution and diffusion analysis were performed. The results show that the viscosity of bio-asphalt is significantly lower than that of base asphalt, and the shear resistance becomes lower at high temperature. In terms of adhesion, bio-asphalt has better temperature sensitivity. The two bio-asphalts have better adhesion than base asphalt and silica at different temperatures, especially at high temperature (65 °C). There was no significant difference between the adhesion energy of the two bio-asphalts. Bio-asphalt is more affected by water intrusion, and its ability to resist water damage is significantly weaker than that of base asphalt. The NPT density-time curve, concentration distribution and MSD calculation results all showed that the self-healing performance of bio-asphalt was better than that of base asphalt, while the two bio-asphalts showed little difference in healing performance.

Keywords:

Bio-asphalt, interfacial adhesion, Self-healing performance, Molecular simulation.

1. Introduction

More and more highways are utilizing asphalt pavement due to its driving comfort, which greatly increases the consumption of asphalt materials in pavement construction and maintenance. At the same time, the non-renewable problem of petroleum and the adverse effects of the extensive use of petroleum asphalt on air, water and soil will restrict the development of the pavement industry [1-4]. Therefore, it is urgent to find new materials to partially or completely replace petroleum asphalt. At present, the extraction of new bio-asphalt materials from renewable energy sources has become the focus of research in the field of pavements. Bio-asphalt is a combination of bio-oil prepared from biomass refining and petroleum asphalt under certain conditions, or by mixing bio-oil with other admixtures under certain conditions, and its biomass sources include forest resources, municipal refuse and animal excrements, have the characteristics of wide source, low cost, green, pollution-free and renewable [1, 3, 5]. Bio-asphalt is mainly used in three ways: directly replaces asphalt binder (100% replacement), using as an asphalt additive (25% to 75% replacement), using acts as an asphalt modifier (<10% % substitution) [6, 7]. On the one hand, the application of bio-asphalt reduces the amount of petroleum asphalt and reduces environmental pollution. On the other hand, the production cost of bio-asphalt is much lower than that of petroleum asphalt which reduces the cost of pavement and is economic beneficial. Sun et al. [8] used waste edible oil as raw material to produce bio-oil, and mixed it with petroleum asphalt at a dosage of 0-8% to prepare bio-asphalt. It was found that the softening point and viscosity of petroleum asphalt decreased after the addition of bio-oil, and the needle penetration and ductility of petroleum asphalt increased, the thermal storage stability was good, the compatibility and low-temperature performance was good, but the high-temperature performance dropped. Min He et al. [9] compared and analyzed the differences in the properties of bio-asphalt prepared from three wood bio-oils: pine, willow, and poplar. They proved that the chemical composition of bio-asphalt prepared from different sources of bio-oil is significantly different, but the thermal storage stability and high-temperature performance are all relatively good, and there is less impact on low-temperature performance. When replacing original asphalt with other materials such as bio-asphalt, the most concern is that if the durability of the asphalt mixture can be guaranteed, such as it's resistance to rutting, water damage and fatigue cracking. Studies have shown that due to the repeated action of vehicle loads and the combined action of climate changes such as oxygen and rain, the kinetic water generated on the pavement will continuously scour and peel off the mixture in the voids of the asphalt surface layer, resulting in local loosening, falling off, potholes of asphalt pavement[10, 11]. The internal cause of looseness and water damage is the insufficient bonding between asphalt and aggregate [12]. The adhesion between asphalt and aggregate is the ability of asphalt film on aggregate surface to resist spalling and damage, which is directly related to the structural strength, water stability and other main properties of asphalt mixture. The bonding between asphalt and aggregate is complicated. Under specific temperature and pressure, the asphalt in the state of separation from each other will produce healing behavior, which will restore the bonding force to a certain extent. It is generally believed that the generation of asphalt self-healing behavior is based on the surface energy theory and the wetting mechanism and diffusion theory [13, 14]. Asphalt at the asphalt-aggregate interface or micro-cracks generated by itself, driven by the intermolecular van der Waals force at the crack interface and the chemical adsorption force formed by hydrogen bonds, in order to reduce the surface energy, the asphalt molecules will gradually diffuse spontaneously. The infiltration and adsorption of the aggregate interface are generated, thereby bridging the micro-cracks between the asphalt and the gap between the asphalt-aggregate interface. Based on the self-healing phenomenon of asphalt, from a macroscopic point of view, micro-cracks in pavement generally decrease during

high temperature in summer. To sum up, it is of great significance to accurately evaluate the bonding performance and healing performance of asphalt mixture for improving the service performance of asphalt pavement, improving the fatigue cracking condition of the road, and prolonging its service life. In recent years, the development of surface technology has helped to better explain the self-healing behavior of asphalt materials at the microscopic level. Among different simulation methods, molecular dynamics (MD) simulation has been proved to be a powerful means to study the physicochemical properties of asphalt materials from a nanoscopic perspective [15-17]. MD simulations can monitor the time-varying motion trajectories of all atoms in the system and provide detailed information to characterize the motion of molecules and their interactions. The simulation output can be linked to its macroscopic properties through statistical mechanics methods. Molecular simulation techniques have been effectively applied to the evaluation of the adhesion properties of asphalt and interfaces and the self-healing properties of asphalt materials [18-20]. Lu and Wang [21, 22] established a molecular model of the asphalt-quartz interface and performed uniaxial tensile and shear test simulations on the interface to explore the stress-strain state and bond failure mechanism of the interface. The results show that the interface failure at low temperature is dominated by the cohesion failure of asphalt, and the presence of interface water molecules can significantly reduce the bond strength between asphalt and aggregates. Xu[23] et al. used molecular simulation to establish the adhesion interface and explored the effect of water on the adhesion performance. They found that the adhesion between SiO2 and asphalt depends on the type of asphalt in the case of low water content. Bhasin[24] pioneered molecular-level research on asphalt self-healing, thus providing a guiding role for subsequent studies of self-healing behavior. In this paper, molecular models of vegetable oil bio-asphalt and waste edible oil bio-asphalt are established based on molecular simulation, and the two bio-asphalt molecular models are verified according to the physical quantities such as density and viscosity. Then, the bio-asphalt-aggregate interlayer model was established, and the adhesion energy and the energy ratio (ER) value under water conditions were calculated and analyzed using energy theory. A bio-asphalt self-healing model was established, and concentration distribution and diffusion analysis were performed. It was intended to evaluate and compare the adhesion and healing behavior of bio-asphalt-aggregates from a molecular perspective.

2. Model Building

2.1. Asphalt Model

The main components of asphalt are saturate, aromatics, resin, and asphaltenes. For the molecular model of asphalt, scholars at home and abroad have successively proposed the asphalt average molecular model, the asphalt three-component model and the asphalt four-component model [25-28]. Asphalt average molecular model is the earliest simplified molecular model proposed based on SHRP-A-675 project, which provides a convenient method for approximating the molecular structure of asphalt. However, the internal structure of the molecular model cannot reflect the actual condition of asphalt, and the interaction information between different components (such as resin, asphaltenes, etc.) cannot be obtained. Therefore, in order to better show the interaction between the various components of asphalt and reflect the diversity of asphalt molecular structure, the multiple components asphalt model came into being and has become the most commonly used simulation model. The three-component model proposed by Greenfield [27] has been used to estimate the basic physical properties of bituminous materials, such as density, glass transition temperature, solubility parameter and modulus. It has good consistency with the experimental data as a whole, which helps researchers to solve many mechanistic problems from a microscopic

perspective, which is of milestone significance. However, there are no polar aromatic components in this model, resulting in inconsistencies between its aromaticity and polarity and the actual asphalt system. From this, a four-component model was proposed [28]. The four-component method can more accurately reflect the properties of actual asphalt molecules, but at the same time, it will increase the workload of simulation calculations. Specifically, this paper adopts a four-component model of twelve molecules to represent the base asphalt, as shown in Figure 1.

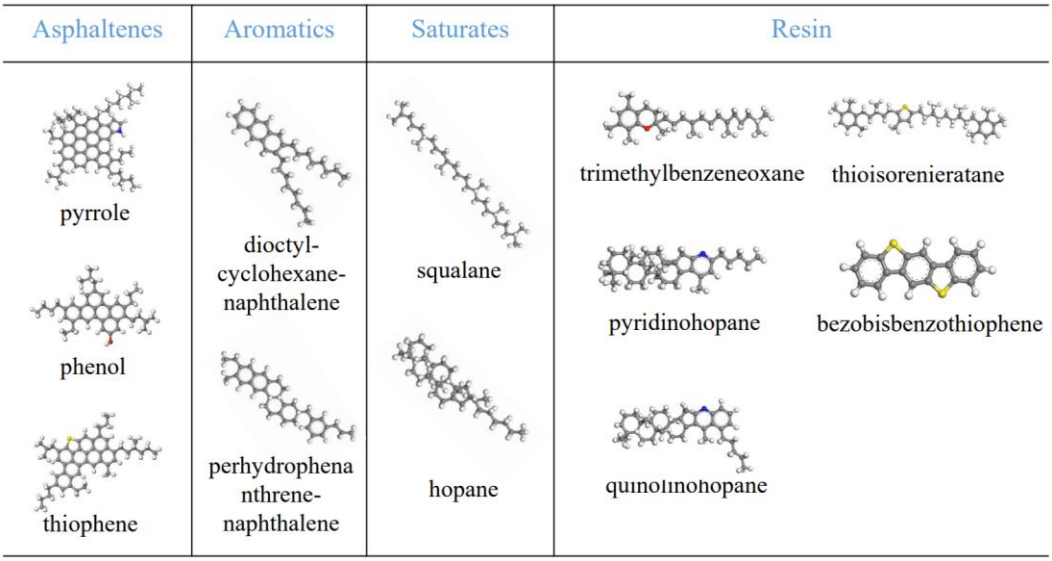

Figure 1. Molecular Model for asphalt

2.2. Molecular Model of Waste Wood–Based Bio Oil (WWO)

The main biomass components of waste wood are lignin and cellulose, and the production of bio-oil is carried out by means of rapid pyrolysis, that is, the biomass material is rapidly heated to high temperature (450-600 °C) in the absence of air. Bio-oil contains a large number of oxygen-enriched organic compounds, mainly including aldehydes, acids, ketones, phenols, etc. [1, 29, 30]. The waste wood biomass oil molecule used in this paper adopts the model proposed by Zhang et al. [31], and the molecular model is shown in Figure 2.

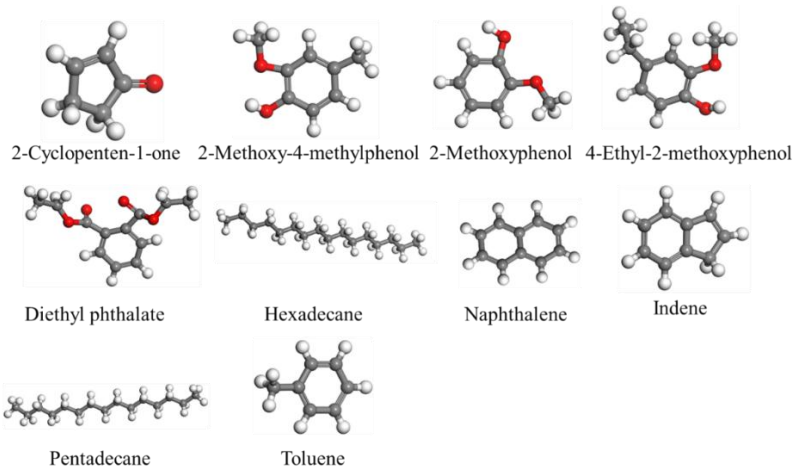

Figure 2. Molecular Model for WWO.

2.3. Molecular Model of Waste Cooking Oil (WCO)

Waste cooking oil (WCO), as a kind of bio-oil, is the waste produced by acidification, hydrolyzation and distillation to extract fatty acids when waste cooking oil is used to refine biodiesel. It contains 60%~70% mixed fatty acids, 5%~10% % of phytosterols and about 5% of vitamins, etc. [32-35], which have great utilization value. The molecular model of waste edible oil used in this paper adopts the model proposed by liu [36], as shown in Figure 3.

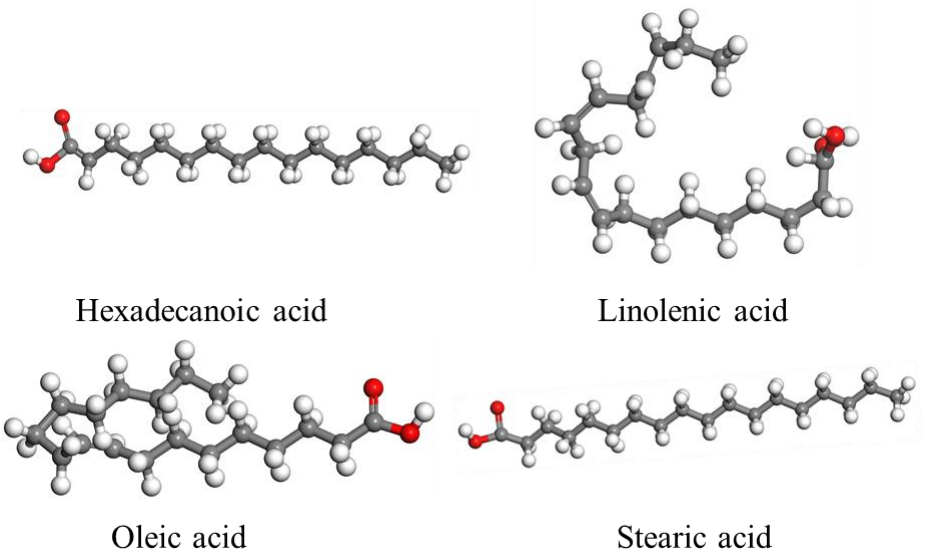

Figure 3. Molecular Model for WCO.

2.4. Model of Bio-asphalt

Bio-asphalt is prepared by mixing bio-oil and asphalt. In this paper, bio-oil is used as an asphalt additive, and the content of bio-oil is about 20%. In this paper, two bio-asphalt models are established, namely waste wood-based bio-asphalt (WWO bio-asphalt) and waste cooking oil-based bio-asphalt (WCO bio-asphalt), and the base asphalt molecules are also established. The model was used as a control to evaluate the effects of different sources of bio-oil additives on the adhesion and self-healing properties of the asphalt-aggregate interface. The proportion of each component of bio-asphalt is shown in Table 1. The molecular simulation task in this paper is completed by the Large-scale Atomic/Molecular Massively Parallel Simulator (LAMMPS) software package [37]. The initial density was set to 0.5g/cm^3 at room temperature (298.15K) when the model was constructed to prevent entanglement and overlap between molecules. The model then goes through 1000 steps of geometric optimization using the smart optimization algorithm to obtain a molecular-equilibrium geometry. Next, the model was subjected to a 100 ps NVT (N: constant number of particles, V: constant volume, T: constant temperature) ensemble simulation at 298.15 K for further equilibration. Thereafter, the NPT (P: constant pressure) ensemble was applied to simulate 100 Ps at one standard atmospheric pressure to obtain the structure of true density. The density-time curve of bio-asphalt is shown in Fig 4. The results show that the resulting density is very close to the test data (0.971-1.001 g/cm^3). A step size of 1.0 fs was chosen in both NVT and NPT simulations to balance computational efficiency and computational accuracy. The content of Waste Wood–Based Bio Oil in the WWO bio-asphalt is 18.96%, the content of waste cooking oil in the WCO bio-asphalt is 18.68%, and the final model box size is 38.5×38.5×38.5 Å.

Table 1. The proportion of each component of bio-asphalt.

Bio-asphalt composition molecule		WWO bio-asphalt		WCO bio-asphalt		Virgin asphalt	
		Number	Weight ratio(%)	Number	Weight ratio(%)	Number	Weight ratio(%)
WWO	2-Methoxy-4-methylphenol	8	18.96				
	Naphthalene	8					
	2-Methoxyphenol	8					
	Diethyl phthalate	4					
	Pentadecane	4					
	2-Cyclopenten-1-one	1 0					
	Indene	6					
	4-Ethyl-2-methoxyphenol	4					
	Hexadecane	2					
	Toluene	2					
WCO	Hexadecanoic acid			5	18.68		
	Linolenic acid			8			
	Oleic acid			11			
	Stearic acid			3			
Saturate	Squalane	4	9.01	4	9.04	5	12.15
	hopane	4		4		5	
Aromatic	dioctyl-cyclohexane-naphthalene	11	25.85	11	25.94	14	32.05
	perhydrophenanthrene-naphthalene	13		13		16	
Resin	quinolinohopane	4	32.2	4	32.31	5	39.80
	thioisorenieratane	4		4		5	
	trimethylbenzeneoxane	5		5		6	
	pyridinohopane	4		4		5	
	benzobisbenzothiophene	15		15		19	
Asphaltene	asphaltene-phenol	3	13.98	3	14.03	4	17.00
	asphaltene-pyrrole	2		2		2	
	asphaltene-thiophene	3		3		4	

Advance Researches in Civil Engineering
ISSN: 2645-7229, Vol.4, No.2, pages: 24-43

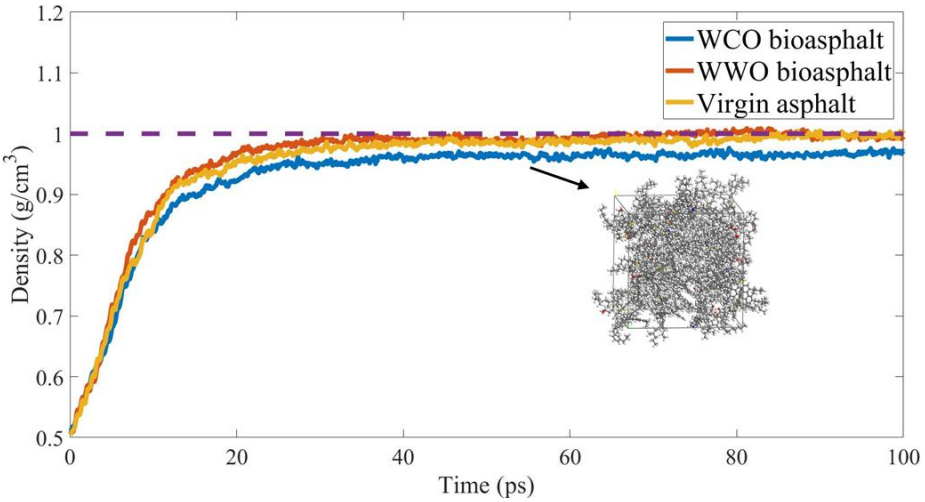

Figure 4. NPT curve for bio-asphalt.

In order to further verify the bio-asphalt model, the physical quantities of glass transition temperature, viscosity, cohesive energy density and solubility parameter were calculated for the established bio-asphalt model. The glass transition temperature is the temperature at which the structure of a polymer material changes from a vitreous state to a highly elastic state. The actual glass transition temperature is not a definite value, but generally refers to a temperature range. The glass transition temperature of a material can be determined experimentally by finding the abrupt range on the temperature-volume or temperature-density curve. Based on this principle, a continuous NPT dynamic simulation was carried out for the heating process (80–500 K, at one standard atmosphere), running for a total of 1 ns. A temperature-volume curve is drawn from the simulated data, and the glass transition temperature value is determined by the trend change of the curve. The simulated Tg results are shown in Figure 5 and Table 2. The Tg of vegetable oil bio-asphalt is about 315K, and the Tg of waste edible oil bio-asphalt is about 295K, and the results are within the reference value range.

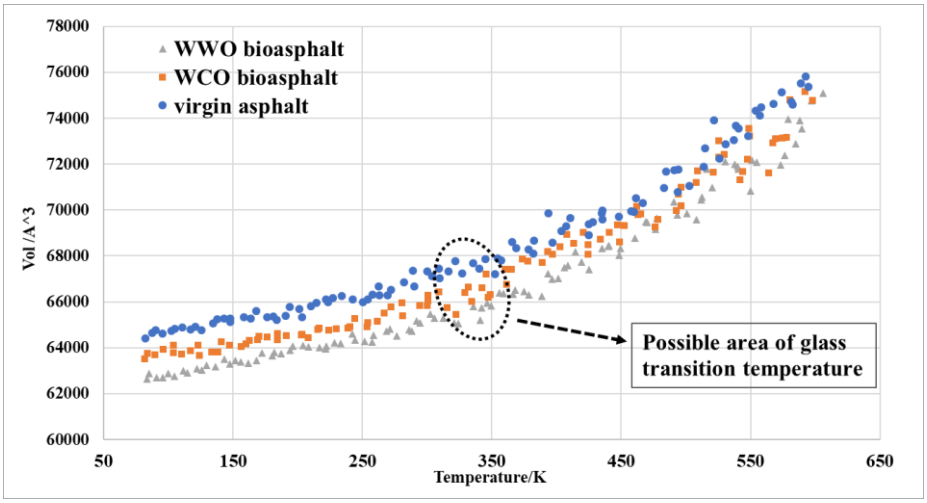

Figure 5. Tg curve for bio-asphalt.

The viscosity of asphalt can evaluate the ability of asphalt material to resist shear deformation under the action of external force, and it is the property most closely related to the mechanical behavior of asphalt pavement. The adhesive properties between bio-asphalt and aggregates can also be directly affected by the viscosity of the asphalt, so it is necessary to calculate the viscosity. Molecular simulations were used to compare the effects of different types of bio-asphalt on viscosity. There are several ways to calculate viscosity using MD: Equilibrium Molecular Dynamics (Green–Kubo and Einstein methods)[38], non-equilibrium MD (NEMD)[39], reverse non-equilibrium MD (rNEMD, also known as Muller-Plathe method)[40]。This paper calculates the viscosity according to the Green-Kubo and Einstein method:

$$\eta = \frac{V}{10k_BT}\int_0^{\infty}\left\langle \sum_{ab} P_{ab}{}^{st}(0)\,P_{ab}{}^{st}(t)\right\rangle dt \tag{1}$$

$$\eta = \lim_{t=\infty}\frac{d}{dt}\frac{V}{20k_BT}\left\langle \sum_{a,b}\left(\Delta A_{ab}(t)\right)^2\right\rangle \tag{2}$$

Where η is the shear viscosity, and V and T are the volume and temperature of the system, respectively. k_B is the Boltzmann constant. $P_{ab}{}^{st}$ is a symmetric traceless pressure tensor element obtained by averaging the instantaneous off-diagonal stress components and then subtracting the pressure from the diagonal components. $\Delta A_{ab}(t) = \int_0^t P_{ab}{}^{st}(t_1)\,dt_1$ represents the stress buildup (essentially the "mean squared displacement" of stress). $\left\langle P_{ab}{}^{st}(0)\,P_{ab}{}^{st}(t)\right\rangle$ is the stress tensor correlation function used to improve convergence. In practice, considering data convergence and computational efficiency, we performed 5 ns EMD simulations on bio-asphalt samples in the NVE ensemble (N: constant number of particles, V: constant volume, E: constant energy). Finally, the viscosity-time curve was drawn, and the average value of the data from 4ns to 5ns was taken as the analysis result. The simulation results are shown in Fig 6 and Table 2, the adhesion of WCO and WWO bio-asphalt is significantly lower than that of base asphalt, which is consistent with the experimental trend [41-43]. The viscosity calculation results are all in the range (1-10 cp) of previous results of using GK to calculate the viscosity of asphalt materials [44-46].

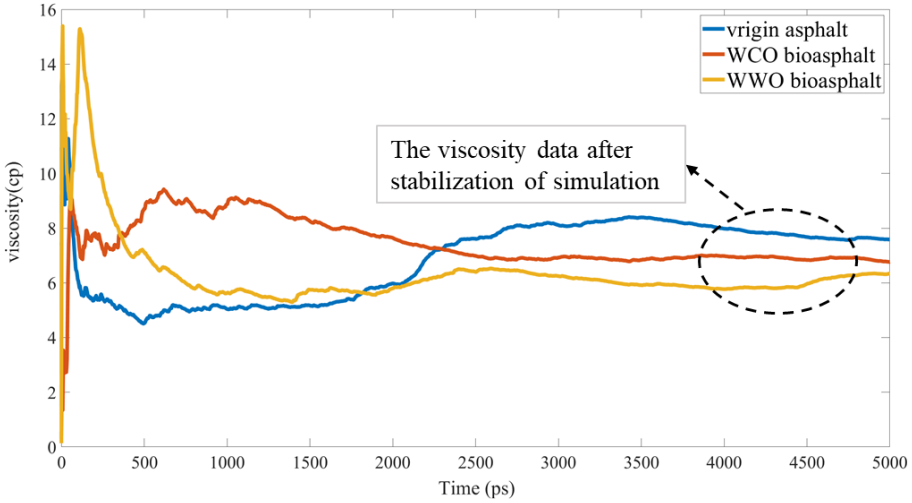

Figure 6. viscosity curve for bio-asphalt.

Cohesive energy is often used to measure the magnitude of the interaction force between macromolecules and is the total energy that a mole of molecules gathers together or expends to separate them. Cohesive energy density is the cohesive energy per unit volume. The solubility parameter δ is a measure of intermolecular forces and a physical constant that measures the compatibility of liquid materials. Its physical meaning is the square root of the cohesive energy density of the material:

$$E_{coh} = [E_{inter}] = [E_{total}] - [E_{intra}] \quad (3)$$

$$CED = E_{coh} / V \quad (4)$$

$$\delta = \sqrt{CED} \quad (5)$$

Where E_{inter} is the total energy between all molecules, E_{total} is the total energy of the entire system, E_{intra} is the intramolecular energy, E_{coh} is the cohesive energy of a molecular system, CED is the cohesive energy density, and δ is the solubility parameter. The calculation results of solubility parameters and cohesive energy density are shown in Table 2, which are all within the reference value range, which proves that the bio-asphalt molecular model established above is reliable and can be used for interface model research.

Table 2. Thermodynamic properties of bio-asphalt molecular models.

Model / Property	WWO bio-asphalt	WCO bio-asphalt	Base asphalt	Reference
Density (g/cm^3)	0.995	0.971	1.001	1.98-1.022[47]
Glass Transition Temperature (K)	Around 320-315K	Around 320-295K	Around 320K	223-303[48], 298.15-358.15[27]
CED (J/m^3)	3.31e+008	3.22e+008	3.323e+008	3.19-3.32 e+008[47]
Solubility Parameter (J/cm^3)$^{0.5}$	18.18	17.995	18.229	13.3-22.5[47]
Viscosity cp）	6.029	6.898	7.729	1-10[44-46]

2.5. Model of Aggregates

At present, the aggregates in the road are mainly acidic aggregates, and the components of the aggregates include SiO_2, Al_2O_3, Fe_2O_3, etc., of which SiO_2 is the main component. In this paper, silica is used as a model for aggregates. The molecular model data is taken from the COD crystal database, and the unit cell structure parameters are a=4.909996 Å, b=4.90996 Å, c=5.402 Å, α=90°, β=90°, γ=120°. In order to more realistically simulate the crystal structure, the silicon dioxide units need to be processed to create a supercell structure. First, the silicon dioxide unit is cut in the [0, 0, 1] direction, and then an 8 × 8 supercell structure is constructed in the x and y directions, with a size of 38 × 38 × 25 Å and an angle of a=β=γ=90°. After that, a vacuum plate with a thickness of 1 Å is added to give the supercell structure a 3D periodic boundary condition. Finally, hydroxyl groups (-OH) were added to the surface of the supercell to show the hydroxylation of silica [49]. The final supercell structure is shown in Figure 7.

Advance Researches in Civil Engineering
ISSN: 2645-7229, Vol.4, No.2, pages: 24-43

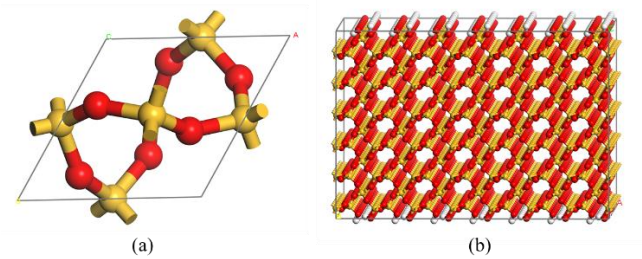

Figure 7. Molecular structure (a) and unit supercell (b) of silica.

3. Calculation Method

Adhesion plays a crucial role in the performance of asphalt concrete, because interfacial spalling and weakening can cause various types of damage, resulting in undesirable diseases such as cracks, potholes, cracks, and ruts in asphalt pavements. Molecular simulations can describe the bonding strength between material interfaces based on energy theory. This paper investigates the adhesion between bio-asphalt and aggregates as a function of temperature and moisture content. The formula for calculating the interfacial energy is as follows [50]:

$$W_{adhension} = \frac{E_{interface} - \left(E_{asphalt} + E_{aggregate}\right)}{A} \tag{6}$$

Where $W_{adhension}$ is the adhesion energy between asphalt and aggregate, $E_{asphalt}$ is the energy of bio-asphalt, $E_{aggregate}$ is the energy of aggregate, $E_{interface}$ is the energy of asphalt-aggregate interface system, and A is the contact area between asphalt and aggregate. A is considered here to eliminate the influence of the interface model size on the adhesion energy. The greater the negative value of $W_{adhension}$, the greater the interaction between the bio-asphalt and the aggregate, and the stronger the adsorption of the bio-asphalt on the aggregate surface. When water enters the asphalt pavement structure from gaps or other channels, the adhesion between asphalt and aggregate will decrease, and long-term contact asphalt will peel off the surface of aggregate. In addition, the effects of traffic loads can generate hydrodynamic pressure, causing asphalt to spall. Eventually, the road will appear loose, peeling, potholes and other diseases. Therefore, it is very necessary to study the water damage resistance between asphalt and aggregate. Thin layers of 100, 300 and 500 water molecules were added to the bio-asphalt-silica interface to discuss the effect of moisture on the interfacial adhesion strength. Debonding energy and Energy ratio (ER) [50] were calculated here to characterize the water damage resistance of CTAC bio-asphalt:

$$W_{debonding} = \frac{\left(E_{as-wa} + E_{agg-wa} - E_{agg-as}\right)}{A} \tag{7}$$

Where $W_{debonding}$ is the work done by the energy when the asphalt is peeled off from the aggregate; $E_{as\text{-}wa}$ is the interface energy between the bio-asphalt and water; $E_{agg\text{-}wa}$ is the interface energy between the aggregate and water; $E_{agg\text{-}as}$ is the interface energy between bio-asphalt and aggregate, and A is the contact area between bio-asphalt and aggregate.

$$ER = \left| \frac{W_{adhension}}{W_{debonding}} \right| \tag{8}$$

The higher the ER value, the stronger the water damage resistance of CTAC bio-asphalt. The specific molecular simulation process is as follows: After the energy optimization, the Nosé-Hoover method is used to perform the NVT molecular simulation with a time step of 1.0 fs and a simulation duration of 100 ps. After the system reached a stable temperature and energy balance, the last 30 frames of the trajectory file were selected to calculate the average adhesion energy. In order to study the self-healing efficiency of different kinds of bio-asphalt, mean square displacement MSD analysis was carried out. For a system in equilibrium, the particles will move according to the force field, and the particles will generally disperse from their initial position. MSD represents the mean square of particle displacement relative to its initial position. MSD describes particle mobility over time and measures the average distance traveled by the molecule. For a system in equilibrium, particles will move according to the applied force and tend to spread out from their original positions. The mean square displacement (MSD) of the particles during the molecular dynamics simulation represents the movement of the asphalt molecules. The increase in MSD over time is related to the diffusion coefficient D, which can be written as:

$$D = \frac{1}{6} \lim_{t \to \infty} \frac{d}{dt} \sum_{i=1}^{N_\alpha} \left\langle \left[r_i(t) - r_i(0) \right]^2 \right\rangle \tag{9}$$

Where $r_i(t)$ is the position vector of particle i at time t. The limiting slope of the MSD as a function of time can be used to estimate the diffusion coefficient of particles. In general, the diffusion coefficient can be simplified to:

$$D = \frac{a}{6} \tag{10}$$

Where a is the slope of the straight line fitting the MSD to the simulation time. The unit is $Å^2/ps$ (or $10^{-4} cm^2/s$).

4. Results Analysis

4.1. The Effect of Temperature on the Bond Strength of Bio-asphalt-aggregate Interface

The effect of temperature on the bond strength of bio-asphalt-aggregate interface obtained by MD simulation is shown in Fig 8. It can be seen from Fig 8 that the bonding energy of the bio-asphalt-aggregate interface varies from -248.95mj/m^2 to -274.96mj/m^2 when the temperature is 5°C to 65°C in this study. This range is consistent with the variation range of adhesion work obtained by macroscopic experiments based on surface energy theory (-110~-358 mj/m^2) [51-56], indicating that the MD simulation results in this study are reasonable. It can be seen from Fig 8 that the adhesion energy between the base asphalt and silica decreases with the increase of temperature, indicating that the base asphalt is significantly affected by temperature. In contrast, the adhesion energy between the two bio-asphalts and silica has no obvious monotonic downward trend, reflecting the better temperature sensitivity of bio-asphalt, which is consistent with the experimental results [57]. At the same time, at different temperatures, especially at high

temperature (65 °C), the two bio-asphalts have better adhesion than base asphalt and silica, which is also consistent with the conclusion obtained from the experiment [58]. In fact, the adhesion between bio-asphalt and aggregates is directly related to the content of bio-asphalt. The bio-asphalt model established in this paper is about 20%. The work of Fayzrakhmanova et al. [59] found that the content of about 20% has a better adhesion. Some scholars have also found that the incorporation of bio-asphalt will reduce the adhesion energy [60, 61]. The possible explanation is that the incorporation of bio-oil increases the proportion of acidic substances in asphalt, and the chemical reaction degree of bio-asphalt on the granite surface decreases, resulting in a decrease in adhesion. The reason for this contradiction may be the difference in the source and composition of bio-asphalt materials. In this paper, molecular simulation is used to model and calculate the main components of vegetable oil and waste edible oil, which provides a reference for the analysis of adhesion between bio-asphalt and aggregates.

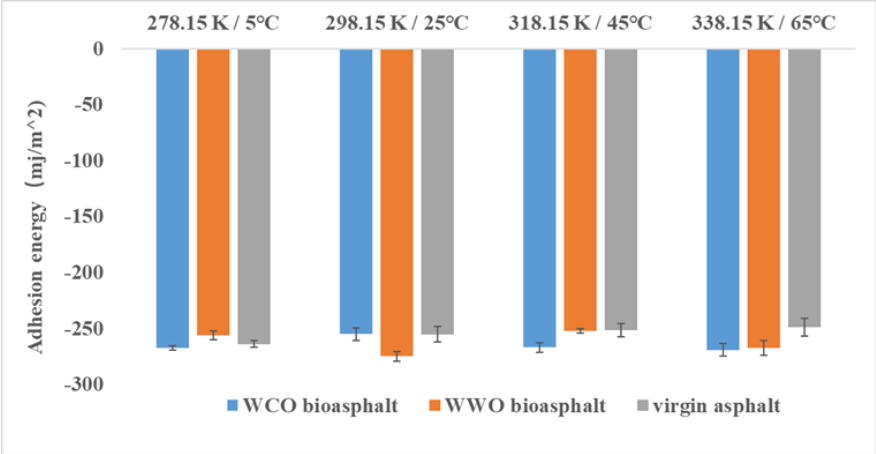

Figure 8. Effect of temperature on adhesion energy of bio-asphalt-silica interface.

4.2. Adhesion State between Bio-asphalt and Aggregate under the Action of Water

According to the calculation formulas of debonding energy and energy ratio described in Section 2.0, the bio-asphalt-water-aggregate model was simulated at 100ps under NVT equilibrium in the molecular simulation, and the energy calculation of the structure was carried out after reaching the equilibrium state, and the results were as follows Fig 9 and Figure 10. When the energy ratio value is larger, the structure is more resistant to water damage. The calculated energy ratio in Fig 10 ranges from 0.5 to 2.5, which is in good agreement with the experimental data [59, 60, 62, 63]. It can be seen from Fig 10 that when the water content between the interfaces increases from 100 water molecules to 300 water molecules (when the water content increases from 1.972% to 5.691%), the energy ratio of the bio-asphalt decreases to an average of about 0.7, which is roughly reduced doubled. When the water content between the interfaces increases from 200 water molecules to 500 water molecules (when the water content increases from 5.691% to 9.138%), the energy ratio value further decreases. It should be noted that when the energy ratio is less than 0.5, it is generally considered that the structure has poor resistance to water damage [62]. Comparing the decrease of the ER values of the three asphalt models during the increase of water molecules, it can be seen that the bio-asphalt is more affected by water intrusion, and the ER values of the bio-asphalt models under the three water contents are all lower than the ER values of the base asphalt model, indicating that the bio-asphalt is weaker than that of base asphalt, which is consistent with the experimental conclusions [59, 60]. When the number of water molecules reaches 300 (9.138%),

the ER value of the base asphalt decreases from 2.5 to 1.2, indicating that the moisture content increases, and even the base asphalt, the ability to resist water damage is greatly weakened. Measures need to be taken, such as adding modifiers, to ensure the adhesion of the bio-asphalt-aggregate interface, resulting in better resistance to water damage.

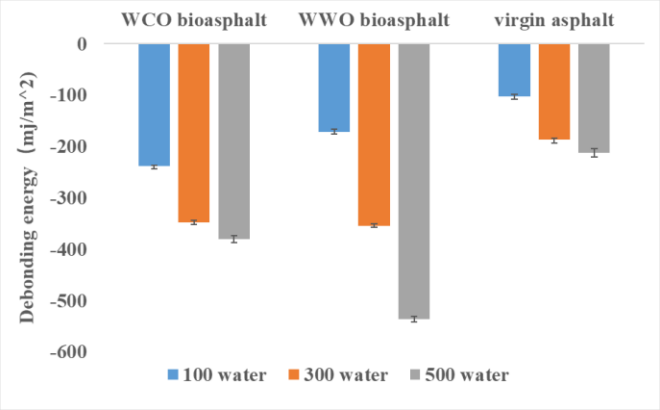

Figure 9. Effect of water content on debonding energy of bio-asphalt-water-silica interface.

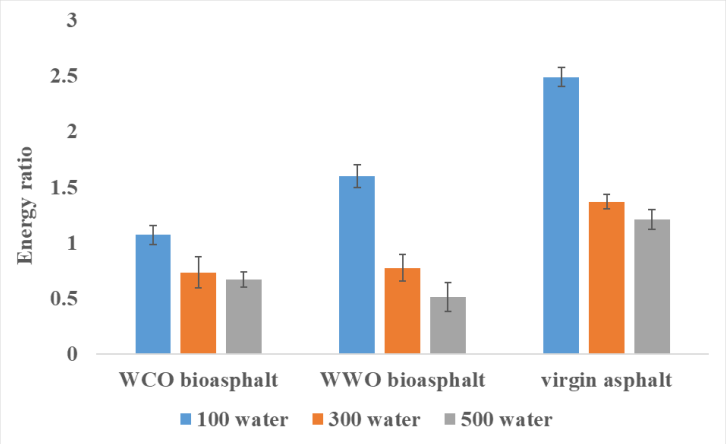

Figure 10. Effect of water content on energy ratio of bio-asphalt-water-silica interface.

4.3. Diffusion Results of Bio-asphalt Self-healing Model

After the molecular dynamics simulation, the bio-asphalt molecules diffused at the artificial crack interface, and the healing of the crack can be observed. The change of the model density with time during the NPT process is shown in Fig 11. As shown in Fig 11, under the condition of one atmospheric pressure, the original 10Å crack thickness in the model is continuously reduced, and it is shown that the asphalt at both ends is close to each other. In the 0-40ps time period, the healing process is relatively fast, and it gradually stabilizes after 40ps. In comparison, WWO and WCO have almost overlapping time-density curves, indicating that the self-healing process and rate of the two are very close. From the 0-20ps density rising section, the slopes of the two bio-asphalt curves are obviously higher than that of the base asphalt. It shows that the self-healing performance of bio-asphalt is better than that of base asphalt, which is also consistent with the conclusions obtained from experiments [13, 14].

Advance Researches in Civil Engineering
ISSN: 2645-7229, Vol.4, No.2, pages: 24-43

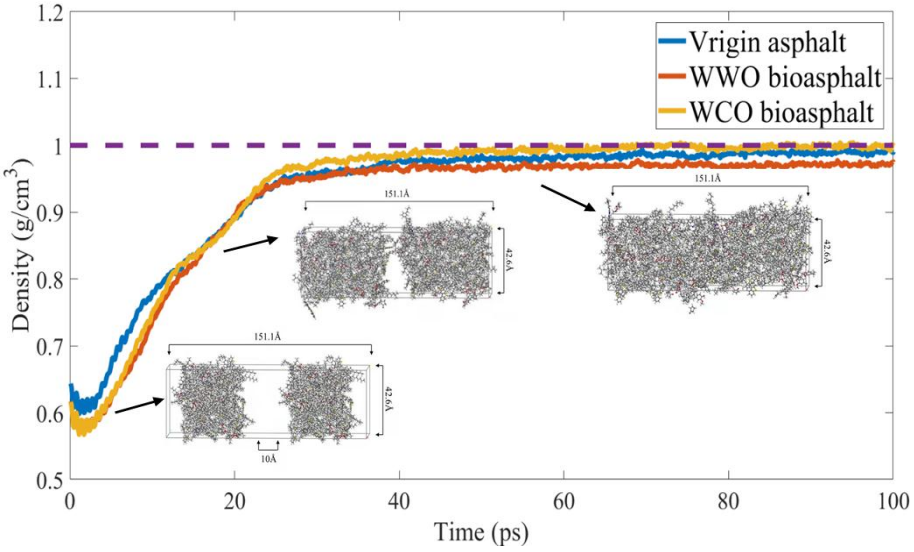

Figure 11. NPT curve for self-healing models of bio-asphalt.

The self-healing ability of bio-asphalt is better than that of base asphalt, which can be explained from the perspective of viscosity. According to the experiment and the simulation data in this paper, it can be known that bio-asphalt has a smaller viscosity, which means greater fluidity. When cracks occur, the ability of bio-asphalt to repair and fill cracks autonomously is stronger. The following is a quantitative evaluation of the self-healing performance of bio-asphalt based on the mean variance displacement and OZ-direction concentration profile. As shown in Figure 12, the bio-asphalt mean variance displacement over time is given. Perform linear fitting on the 0-20ps and 20-50ps results, respectively, to obtain the slope of the fitted line, and multiply by one-sixth to obtain the diffusion coefficient. The results are listed in Table 3 below.

Table 3. Diffusion coefficient for self-healing models of bio-asphalt.

		Virgin asphalt	WCO bio-asphalt	WWO bio-asphalt
0-20ps	slope a	1.1143	1.5886	1.5408
	Diffusion coefficient D	0.185717	0.264767	0.2568
20-50ps	slope a	0.7104	0.7725	0.914
	Diffusion coefficient D	0.1184	0.12875	0.152333

From the value of the diffusion coefficient D, the self-healing ability of bio-asphalt can be more intuitively and quantitatively evaluated. It can be seen from the data that the diffusion of bio-asphalt is better than that of base asphalt. This can be judged from the numerical value of the diffusion coefficient, in which the WCO bio-asphalt diffuses the fastest in the 0-20ps time period, reaching 0.264767Å^2/ps, and the 20-50ps time period WWO bio-asphalt diffusion is the fastest, reaching 0.152333Å^2/ps. correspondingly, the base asphalt diffusion coefficients are only 0.185717Å^2/ps and 0.1184Å^2/ps. This is consistent with the conclusions obtained from the NPT time-density curve. At the same time, it is noted that the MSD curve turns around 20ps, which may be caused by the rapid filling of the cracked area with asphalt in the self-healing model in the time period of 0-20ps, and the slow healing process of small volume after 20ps.

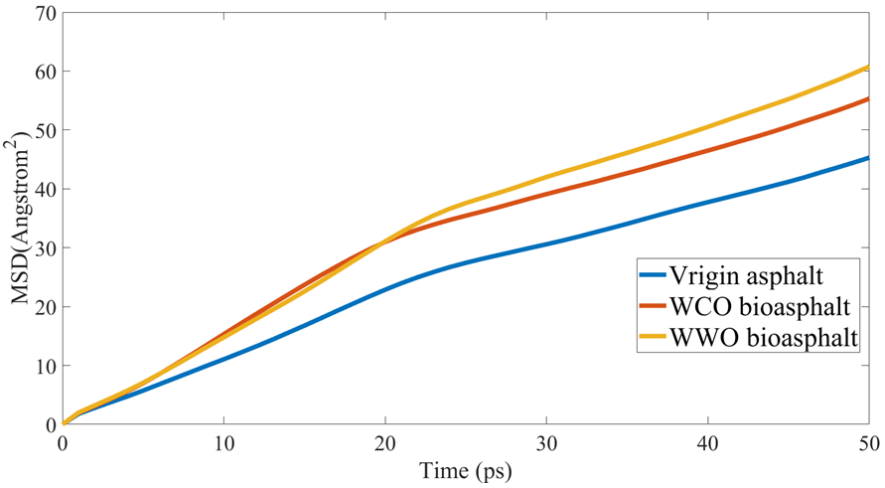

Figure 12. MSD curve for self-healing model of bio-asphalt.

Through the concentration statistics of the crack model, the relative concentration data in the OZ direction can be obtained, as shown in Figure 13. In order to highlight and compare the self-healing efficiency of the three asphalt models, considering that the four models have completed diffusion healing at 50 ps, the data at five time points of 0, 25, 50, 75, and 100 ps were selected for model OZ concentration analysis. It can be seen from Fig 13 that the relative concentration values in the middle 60-70 Å of the three asphalt self-healing models are all 0 at 0 ps, which corresponds to the existence of the middle crack region at the beginning of the model. Under the condition of 298K normal temperature and one atmospheric pressure, the relative concentration in the crack area gradually increases with time, which indicates that the asphalt at both ends of the model gradually moves closer under the interaction to heal the middle crack area. The WWO and WCO models were supplemented at 25 ps in the crack region concentration and reached a relatively average state at 50 ps. In comparison, the concentration concave in the crack area is still obvious when the base asphalt is 25ps, and the concentration in the crack area fluctuates significantly at 50ps, which does not reach a relative average. This intuitively shows that the healing speed of base asphalt is slower than that of bio-asphalt, reflecting the excellent healing performance of bio-asphalt. Comparing the concentration distribution curves of WWO and WCO, no obvious concentration difference was found at different times, and they reached a relatively even distribution state at 50ps, indicating that the healing has been completed, and there is almost no difference in the healing performance of the two bio-asphalts. This is consistent with the conclusions obtained from the previous density-time curves and MSD curves.

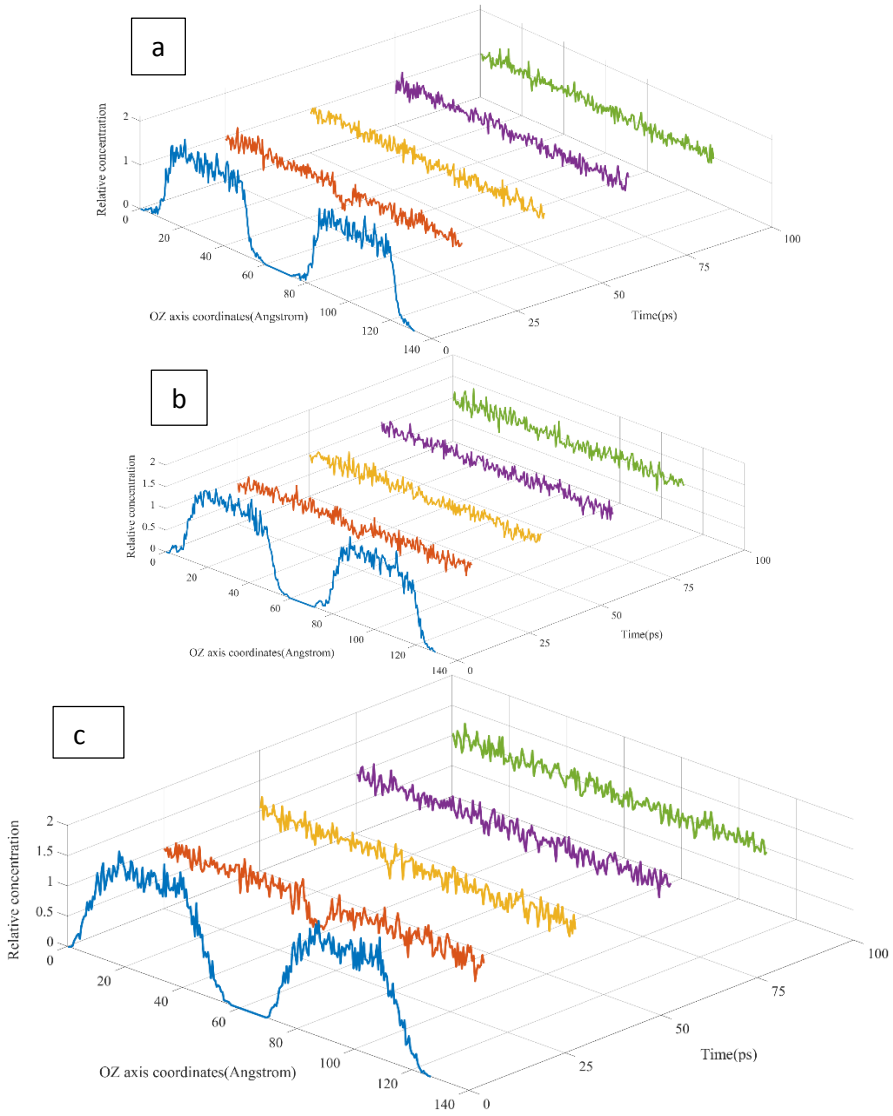

Figure 13. Concentration varying with time along OZ direction for self-healing models bio-asphalt (a)WWO bio-asphalt (b) WCO bio-asphalt (c) Virgin asphalt.

5. Conclusions

In this paper, the molecular dynamics method was used to evaluate and compare the bio-asphalt-aggregate adhesion effect. Firstly, the molecular model of bio-asphalt was established, and the molecular model was verified according to the physical quantities such as density and solubility parameters. At the same time, the bio-asphalt-aggregate interlayer model was established, the adhesion energy and ER value were calculated and analyzed by using energy theory, the bio-asphalt self-healing model was established, and the concentration distribution and diffusion analysis were carried out. The conclusions are as follows:

(1) The validation parameters of the established bio-asphalt model are all within the reference value range, which proves that the established model is reliable and can be used in the study of adhesion and healing behavior in this paper. At the same time, the viscosity calculation results show that the

viscosity of the bio-asphalt is significantly lower than that of the base asphalt, and the shear resistance becomes lower at high temperature, which is consistent with the experimental results.
(2) The calculation results of the adhesion energy at different temperatures show that the base asphalt is significantly affected by temperature. In comparison, the bio-asphalt has better temperature sensitivity, which is consistent with the experimental results [57]. The two kinds of bio-asphalt had better adhesion between the base asphalt and silica at different temperatures, especially at high temperature (65℃). There was no obvious difference between the two bio-asphalt adhesion energies. Bio-asphalt is more affected by water intrusion, and the ER values of bio-asphalt models at three water contents are all lower than the ER values of base asphalt models, indicating that bio-asphalt has weaker resistance to water damage than base asphalt.
(3) NPT density time curve, concentration distribution and MSD calculation results all show that the self-healing performance of bio-asphalt is better than that of base asphalt. There was little difference in healing properties between the two bio-asphalts.

6. References

[1]- Raman, N. A. A., et al., 2015, **A review on the application of bio-oil as an additive for asphalt**, International Journal of Pavement Engineering , 72(5), 24-35.
[2]-Azahar, W. N. A. W., et al., 2016, **The potential of waste cooking oil as bio-asphalt for alternative binder â€“An overview**, International Journal of Pavement Engineering **,** 78(4), 130-145.
[3]-Peralta, J., et al., 2013, **Development of an innovative bio-binder using asphalt-rubber technology**, International Journal of Pavement Engineering, 80(4), 202-215.
[4]-Movilla-Quesada, D., et al., 2017, **Reduction in the use of mineral aggregate by recycling cellulose ashes to decrease the aging of hot asphalt mixtures**, International Journal of Pavement Engineering, 143, 547-557.
[5]-Mousavi, M., et al., 2016, **Multiscale investigation of oxidative aging in biomodified asphalt binder**, International Journal of Pavement Engineering, 120(31), 17224-17233.
[6]-Raouf, M. A., Metwally, M. and Williams, R. C., 2010, **Development of non-petroleum based binders for use in flexible pavements**, International Journal of Pavement Engineering.
[7]-Raouf, M. A., Williams, C. R. J. R. M. and Design, P., 2010, **General rheological properties of fractionated switchgrass bio-oil as a pavement material**, International Journal of Pavement Engineering, 11, 325-353.
[8]-Sun, Z., et al., 2016, **Properties of asphalt binder modified by bio-oil derived from waste cooking oil**, International Journal of Pavement Engineering**,** 102, 496-504.
[9]- He, M., et al., 2019, **Comparative analysis of bio-binder properties derived from different sources**, International Journal of Pavement Engineering, 20(7), 792-800.
[10]-Anderson, D., et al., 1988, **More effective cold, wet weather patching materials for asphalt pavements**.
[11]- Anderson, D. A. and Thomas, H. R., 1984, Pothole repair in Pennsylvania.
[12]-Wilson, T. and T. Wilson, 1998, **Long-Term Monitoring of Pavement Maintenance Materials Test Sites**, United States. Federal Highway Administration.
[13]-Sun, G., et al., 2021, **Roles of aging and bio-oil regeneration on self-healing evolution behavior of asphalts within wide temperature range**, Journal of Cleaner Production, 329, 129712.
[14]-Norambuena-Contreras, J., et al., 2020, **Microencapsulated bio-based rejuvenators for the self-healing of bituminous materials**, Materials, 13(6), 1446.

[15]-Zhang, L. and Greenfield, M. L., 2007, **Analyzing properties of model asphalts using molecular simulation**, Energy and fuels, 21(3), 1712-1716.
[16]-Xu, G. and Wang, H., 2016, **Study of cohesion and adhesion properties of asphalt concrete with molecular dynamics simulation**, Computational Materials Science, 112, 161-169.
[17]-Xu, G. and Wang, H., 2016, **Molecular dynamics study of interfacial mechanical behavior between asphalt binder and mineral aggregate**. Construction and Building Materials, 121, 246-254.
[18]-Sun, D., et al., 2016, **Indices for self-healing performance assessments based on molecular dynamics simulation of asphalt binders**, Computational Materials Science, 114, 86-93.
[19]-Shen, S., et al., 2016, **Investigation of the influence of crack width on healing properties of asphalt binders at multi-scale levels**. Construction and Building Materials, 126, 197-205.
[20]-He, L., et al., 2020, **Self-healing behavior of asphalt system based on molecular dynamics simulation**, Construction and Building Materials, 254, 119225.
[21]-Lu, Y. and L. J. I. J. O. P. E., Wang, 2011, **Nano-mechanics modelling of deformation and failure behaviours at asphalt–aggregate interfaces**, International Journal of Pavement Engineering, 12(4), 311-323.
[22]-Lu, Y., and L. J. I. J. O. P. E., Wang, 2010, **Nanoscale modelling of mechanical properties of asphalt–aggregate interface under tensile loading**, International Journal of Pavement Engineering, 11(5), 393-401.
[23]-Wang, H., Lin, E., and Xu,G., 2017, **Molecular dynamics simulation of asphalt-aggregate interface adhesion strength with moisture effect**, International Journal of Pavement Engineering, 18(5), 414-423.
[24]-Bhasin, A., et al., 2011, **Use of molecular dynamics to investigate self-healing mechanisms in asphalt binders**, Journal of Materials in Civil Engineering, 23(4), 485-492.
[25]-Hansen, J. S., et al., 2013, **Four-component united-atom model of bitumen**, The Journal of chemical physics, 138(9), 094508.
[26]-Li, D. D. and Greenfield, M. L., 2014, **Chemical compositions of improved model asphalt systems for molecular simulations**, Fuel, 115, 347-356.
[27]-Zhang, L. Q. and Greenfield, M. L., 2007, **Relaxation time, diffusion, and viscosity analysis of model asphalt systems using molecular simulation**, Journal of Chemical Physics, 127(19), 13.
[28]-Zhang, L. and Greenfield, M. L., 2008, **Effects of polymer modification on properties and microstructure of model asphalt systems**, Energy & Fuels, 22(5), 3363-3375.
[29]-Yang, X., et al., 2014, **Mechanical performance of asphalt mixtures modified by bio-oils derived from waste wood resources**, International Journal of Pavement Engineering, 51, 424-431.
[30]-Zhang, R., et al., 2018, **Using bio-based rejuvenator derived from waste wood to recycle old asphalt**, Journal of Materials in Civil Engineering, 189, 568-575.
[31]-Zhang, R., et al., 2020, **Modification mechanism of using waste wood–based bio-oil to modify petroleum asphalt**, Journal of Materials in Civil Engineering, 32(12), 04020375.
[32]-Yang, X., J. Mills-Beale, and Z. J. J. O. C. P., You, 2017, **Chemical characterization and oxidative aging of bio-asphalt and its compatibility with petroleum asphalt**, Journal of Materials in Civil Engineering, 142, 1837-1847.
[33]-Yang, X., Z. J. C., You, 2015, **Materials, High temperature performance evaluation of bio-oil modified asphalt binders using the DSR and MSCR tests**, Journal of Materials in Civil Engineering, 76, 380-387.

[34]-Zhang, D., et al., 2017, **Analysis of the relationships between waste cooking oil qualities and rejuvenated asphalt properties**, Journal of Materials in Civil Engineering, 10(5), 508.
[35]-Seidel, J. C., and J. E. J. A. B. f. S. A. P. W. D., Haddock, 2012**, Soy fatty acids as sustainable modifier for asphalt binders**.
[36]-Liu, J. X., 2018, **Component of Waste Cooking Oil Based on Molecular Weight Classification and Its Effect on Performance of Aging Asphalt**, Wuhan University of Technology, Wuhan, China.
[37]-Thompson, A. P., et al., 2022, **LAMMPS-a flexible simulation tool for particle-based materials modeling at the atomic, meso, and continuum scales**, Computer Physics Communications, 271, 108171.
[38]-Mondello, M. and Grest, G. S., 1997, **Viscosity calculations of n-alkanes by equilibrium molecular dynamics**, The Journal of chemical physics, 106(22), 9327-9336.
[39]-Evans, D. J. and Morriss, G., 1984, **Nonlinear-response theory for steady planar Couette flow**, Physical Review A, 30(3), 1528.
[40]-Müller-Plathe, F., 1995, **Reversing the perturbation in nonequilibrium molecular dynamics: An easy way to calculate the shear viscosity of fluids**, Physical Review E, 59(5), 4894.
[41]-Wan Azahar, W. N. A., et al., 2014, **Performance of waste cooking oil in asphalt binder modification**, in Key Engineering Materials, Trans Tech Publication.
[42]-Mills-Beale, J., et al., 2014, **Aging influence on rheology properties of petroleum-based asphalt modified with biobinder**, Journal of Materials in Civil Engineering, 26(2), 358-366.
[43]-Yang, X., You, Z., and Mills-Beale, J., 2015, **Asphalt binders blended with a high percentage of biobinders: Aging mechanism using FTIR and rheology**, Journal of Materials in Civil Engineering, 27(4), 04014157.
[44]-Zhang, L., and Greenfield, M. L., 2007, **Relaxation time, diffusion, and viscosity analysis of model asphalt systems using molecular simulation**, The Journal of chemical physics, 127(19), 194502.
[45]-Li, D. D. and Greenfield, M. L., 214, **Viscosity, relaxation time, and dynamics within a model asphalt of larger molecules**, The Journal of chemical physics, 140(3), 034507.
[46]-Xu, G. and Wang, H., 2017, **Molecular dynamics study of oxidative aging effect on asphalt binder properties**, Fuel, 188, 1-10.
[47]-Wang, P., et al., 2015, **Investigating the Interactions of the Saturate, Aromatic, Resin, and Asphaltene Four Fractions in Asphalt Binders by Molecular Simulations**, Energy and Fuels, 29(1), 112-121.
[48]-Chu, L., Luo, L., and Fwa, T. F., 2019, **Effects of aggregate mineral surface anisotropy on asphalt-aggregate interfacial bonding using molecular dynamics (MD) simulation**, Construction and Building Materials, 225, 1-12.
[49]-Zhuravlev, L. T., 1987, Concentration of hydroxyl-groups on the surface of amorphous silicas, Langmuir, 3(3), 316-318.
[50]-Bhasin, A., 2007, **Development of methods to quantify bitumen-aggregate adhesion and loss of adhesion due to water**, Texas A&M University.
[51]-Alvarez, A. E., et al., 2019, **Optimising the effect of natural filler on asphalt-aggregate interfaces based on surface free energy measurements**, Road Materials and Pavement Design, 20(7), 1548-1570.
[52]-Arabani, M. and Hamedi, G. H., 2011, **Using the Surface Free Energy Method to Evaluate the Effects of Polymeric Aggregate Treatment on Moisture Damage in Hot-Mix Asphalt**, Journal of Materials in Civil Engineering, 23(6), 802-811.

[53]-Cheng, D. X., et al., 2002, **Surface energy measurement of asphalt and its application to predicting fatigue and healing in asphalt mixtures, in Bituminous Binders**, **Materials and Construction**, Transportation Research Board Natl Research Council: Washington, 44-53.
[54]-Cheng, D., 2002, **Surface free energy of asphalt -aggregate system and performance analysis of asphalt concrete based on surface free energy**, ProQuest LLC.
[55]-Yi, J. Y., et al., 2018, **Studies on surface energy of asphalt and aggregate at different scales and bonding property of asphalt-aggregate system**, Road Materials and Pavement Design, 19(5), 1102-1125.
[56]-Zhai, R. and Hao, P., 2020, **Research on the impact of mineral type and bitumen ageing process on asphalt-mineral adhesion performance based on molecular dynamics simulation method**, Road Materials and Pavement Design, 1-14.
[57]-Gao, J., et al., 2018, **Rheological behavior and sensitivity of wood-derived bio-oil modified asphalt binders**., Applied Sciences, 8(6), 919.
[58]-Girimath, S., Singh, D., and Showkat, B., 2021, **Influence of Bio-oil Modification on Moisture-Induced Damage Potential of Asphalt Binder and Mix**, Advances in Civil Engineering Materials, 10(1), 276-299.
[59]-Fayzrakhmanova, G., et al., 2016, **A study of the properties of a composite asphalt binder using liquid products of wood fast pyrolysis**, Polymer Science Series D, 9(2), 181-184.
[60]-Caro, S., et al., 2016, **Studying the impact of biomodifiers produced from agroindustrial wastes on asphalt binders**, Construction and Building Materials, 2016. 126: p. 369-380.
[61]-Yang, X., et al., 2014, **Mechanical performance of asphalt mixtures modified by bio-oils derived from waste wood resources**, Construction and Building Materials, 51, 424-431.
[62]-Bhasin, A., et al., 2006, **Limits on adhesive bond energy for improved resistance of hot-mix asphalt to moisture damage**, Transportation Research Record, 1970(1), 2-13.
[63]-Collis-George, N. and Figueroa, B., 1984, **The use of high energy moisture characteristic to assess soil stability**, Soil Research, 22(3), 349-356